

Optimal Chance-Constrained Scheduling of Reconfigurable Microgrids Considering Islanding Operation Constraints

Hemmati , Mohammad ; Mohammadi-ivatloo, Behnam; Abapour, Mehdi; Anvari-Moghaddam, Amjad

Published in:
I E E Systems Journal

DOI (link to publication from Publisher):
[10.1109/JSYST.2020.2964637](https://doi.org/10.1109/JSYST.2020.2964637)

Publication date:
2020

Document Version
Accepted author manuscript, peer reviewed version

[Link to publication from Aalborg University](#)

Citation for published version (APA):

Hemmati , M., Mohammadi-ivatloo, B., Abapour, M., & Anvari-Moghaddam, A. (2020). Optimal Chance-Constrained Scheduling of Reconfigurable Microgrids Considering Islanding Operation Constraints. *I E E Systems Journal*, 14(4), 5340-5349. Article 8974607. <https://doi.org/10.1109/JSYST.2020.2964637>

General rights

Copyright and moral rights for the publications made accessible in the public portal are retained by the authors and/or other copyright owners and it is a condition of accessing publications that users recognise and abide by the legal requirements associated with these rights.

- Users may download and print one copy of any publication from the public portal for the purpose of private study or research.
- You may not further distribute the material or use it for any profit-making activity or commercial gain
- You may freely distribute the URL identifying the publication in the public portal -

Take down policy

If you believe that this document breaches copyright please contact us at vbn@aub.aau.dk providing details, and we will remove access to the work immediately and investigate your claim.

Optimal Chance-Constrained Scheduling of Reconfigurable Microgrids Considering Islanding Operation Constraints

Mohammad Hemmati^{ID}, Behnam Mohammadi-Ivatloo^{ID}, *Senior Member, IEEE*, Mehdi Abapour^{ID},
and Amjad Anvari-Moghaddam^{ID}, *Senior Member, IEEE*

Abstract—Microgrid concept is one of the suitable strategies for increasing resilience and preventing load curtailment, especially in emergency conditions. Operation in islanded mode is one of the unique features of microgrids that can provide numerous benefits for both consumers and energy producers. Unlike the conventional distribution networks, reconfigurable microgrids enable the reconfiguration process to achieve optimal structure. In this article, a new optimal strategy for scheduling of reconfigurable microgrids considering islanding capability constraints is presented. To demonstrate the successful islanding operation, the islanding capability is considered as a probability of islanding operation (PIO) index which shows the probability, that the microgrid has adequate level of spinning reserve to meet the local load. Taking into account the forecast errors of generated power by renewable energy resources (PV and wind) as well as load demand, the 13-interval approximation is used for the simplification of nonlinearity of PIO. The scheduling of reconfigurable microgrid with islanding operation constraints is formulated as a chance-constrained goal optimization problem, where the objective is defined as minimizing the total operation cost of microgrid in terms of fuel cost, reliability cost, cost of purchasing power from the mains, and switching cost. The proposed method is implemented on a 10-bus radial reconfigurable microgrid test system with photovoltaic (PV) panels, wind turbines, battery, and microturbines, with different levels of PIO. The numerical results show the effectiveness of the proposed scheduling method.

Index Terms—Chance-constrained goal programming (CCGP), microgrid, probability of islanding operation (PIO), reconfiguration, spinning reserve.

Manuscript received August 17, 2019; revised November 12, 2019; accepted December 7, 2019. (Corresponding author: Behnam Mohammadi-Ivatloo.)

M. Hemmati and M. Abapour are with the Faculty of Electrical and Computer Engineering, University of Tabriz, Tabriz 51666, Iran (e-mail: m.hemmati@tabrizu.ac.ir; abapour@tabrizu.ac.ir).

B. Mohammadi-Ivatloo is with the Faculty of Electrical and Computer Engineering, University of Tabriz, Tabriz 51666, Iran, and also with the Institute of Research and Development, Duy Tan University, Da Nang 550000, Vietnam (e-mail: bmohammadi@tabrizu.ac.ir; mohammadiivatloo@behnam@duytan.edu.vn).

A. Anvari-Moghaddam is with the Department of Energy Technology, Aalborg University, 9220 Aalborg, Denmark (e-mail: aam@et.aau.dk).

Digital Object Identifier 10.1109/JSYST.2020.2964637

NOMENCLATURE

Indices

b	Index of battery storage units.
i	Index of microturbine units.
J	Index of system buses.
k	Index of branches.
L	Index of load.
s	Index of remotely controlled switches.
t	Index of time.

Parameter

C_j^L	Cost of interruption in j th bus.
I_k^{\max}	Maximum current of k th branch.
MUT/MDT	Minimum up/down time.
MD/MC	Minimum discharging/charging time.
$N^{sw,\max}$	Maximum number of switching actions.
$P_{pcc}^{\max}/P_{pcc}^{\min}$	Maximum/minimum power exchanged.
$P_{char_b}^{\min}/P_{char_b}^{\max}$	Minimum and maximum charging power of the b th battery.
$P_{dis_b}^{\min}/P_{dis_b}^{\max}$	Minimum and maximum discharging power of the b th battery.
P_i^{\min}/P_i^{\max}	Minimum/maximum generated power by i th micro-turbine (MT).
PIO^{target}	Target probability for scheduling of microgrid in islanded mode.
RU_i/RD_i	Ramp up/down of the i th MT.
SOC^{\min}/SOC^{\max}	Minimum/maximum state of charge of a battery.
V_j^{\min}/V_j^{\max}	Minimum and maximum voltage of j th bus.

Variables

I_k	Current of the k th branch.
La_j	Average load connected to the j th bus.
N_s^{sw}	Number of switching action of the s th switch.
P_{pcc}	Exchanged power with upstream network.
P_d	Forecasted load demand.
P_w/P_{PV}	Forecasted wind and PV power generation.
P_b	Battery charge or discharge power.
$P_{i,t}$	Generated power by the i th MT at t th time interval.

R_i^d/R_i^u	Down/up spinning reserve of the i th MT.
R_b^d/R_b^u	Down/up spinning reserve of the b th battery.
SOC_b	State of charge of the b th battery.
$S_{s,t}$	Status of the s th switch at t th time interval.
T_i^{on}/T_i^{off}	Number of ON/OFF hours of the i th MT.
T_b^{char}/T_b^{dis}	Number of charge/discharge hours of the b th battery.
V_j	Voltage of the j th bus.
X_b^c/X_b^d	Binary variable for charge/discharge of battery.
$X_{i,t}$	State of the i th MT at t th time interval.

I. INTRODUCTION

THE need for highly reliable and flexible distribution networks is a critical challenge for energy producers and consumers. This problem can be solved by management and scheduling of microgrids, which are key players in active distribution networks. Microgrid is a small or medium-scale distribution network consisting of distributed generation (dispatchable and nondispatchable unit), energy storage system (ESS), controllable load, and switches [1]. Microgrid is connected to the upstream network at the point of common coupling (PCC) and can exchange power with it. One of the significant advantages of microgrids lies within their islanding capability during the disturbance and emergency conditions through which they can secure local loads and improve the system reliability. According to the IEEE.1547.7 standard, the islanded mode can provide several benefits such as reliability and power quality improvement, cost minimization, and ancillary services [2].

Besides the conventional microgrids, reconfigurable microgrids (RMGs), which are deemed as the next-generation of microgrids, have attracted much attention over the past years [3]–[6]. Generally, RMG is a type of microgrid that is equipped with remotely controlled switches (RCSs) (i.e., tie switches and sectionalizers) and is able to provide a flexible structure for rerouting the power throughout the network. In comparison with traditional distribution networks, RMG has more control variables (such as dispatchable units, controllable loads, and RCS) [7]. The reconfiguration capability can facilitate the microgrid scheduling for different goals, such as reliability improvement [8], cost minimization [9], load restoration [10], etc.

Although the microgrid scheduling has been studied widely, most of the studies focus on the microgrid scheduling in connected mode. In [11], microgrid management is presented in a grid-connected mode using reconfiguration and unit commitment. In [12], the problem of integrated heat and power microgrid in the presence of selling/purchasing power price uncertainty is developed. The proposed microgrid contains various types of heat and power generation units and the goal of the article is to find the optimum set points of microgrid components in order to minimize the operation cost. Likewise, in [13], the energy management problem, under uncertainties based on chance-constrained programming for a grid-connected microgrid, is investigated.

Renewable energy sources (RESs) also have a major role in microgrids, however, they could cause power fluctuations. To address the uncertainty caused by these units, the scheduling problem must be investigated by stochastic methods. Three methods, namely, chance-constrained programming, stochastic programming, and robust optimization, are among the most widely used approaches for uncertainty modeling [14], [15]. A scenario-based robust energy management is introduced in [16] for uncertainly handling in worst case. By optimizing the worst case scenario, the microgrid energy management will become robust against the possible realizations of the uncertain parameters which are simulated by Monte Carlo. Authors in [17] take advantages of battery ESSs for providing multiple services to microgrid. Besides introducing an energy management approach for thermal and electrical sources of the studied microgrid, a chance-constrained planning is implemented to handle the load and solar power fluctuations. In [18], a chance-constrained stochastic model for scheduling of microgrid is presented. The uncertainties of RESs and load variation, as well as, the provisional islanding causes by external disturbances are handled by stochastic scenarios and a joint chance-constraint is proposed for controlling the operational risks.

Due to the intermittent and unpredictable nature of RESs, a scenario-robust mixed-integer linear programming is presented for improving the performance of hybrid microgrids [19]. In [20], a chance-constrained information gap decision theory (IGDT) model is proposed by considering two categories of uncertainty for multiperiod scheduling of a microgrid. The chance-constraints are imposed in the operational stage for uncertainty modeling, including hourly generated power of RESs and load variation. In [21], an optimal control strategy is introduced for power flow management in microgrids. Due to different types of uncertainties caused by RESs, load demand, and charging/discharging behaviors of electric vehicles (EVs), the problem is reformulated as a stochastic chance-constrained optimization.

Although microgrid scheduling with different types of uncertainty is reported in the literature, there are few research works which consider the scheduling of microgrids with islanding capability. In [14], a chance-constrained energy management model for an islanding microgrid is developed following the objective of minimizing the generation cost, ESS degradation cost, and emission cost. Generated power by RES is considered as an uncertain parameter and a novel ambiguity set is proposed to capture the uncertainty. In [22], microgrid scheduling with multiperiod islanding constraints is proposed. To identify the microgrid capability in operating in islanded condition, the T - τ criterion is introduced. In [23], mixed-integer linear programming (MILP)-based splitting method is introduced for islanding operation of power system. However, uncertainties in the forecast methods may lead to incorrect decision in energy management system for islanding microgrid. In [24], differences between the actual and predicted data sequence were used to determine compensation of uncertainty associated with PV in islanded microgrid. The probability of successful islanding (PSI) criteria is proposed in [25] to determine the probability of microgrid meeting demands and maintaining a sufficient amount of reserve

TABLE I
COMPARISON OF THE INNOVATIONS OF THIS ARTICLE WITH OTHER WORKS

	Description
Ref [24]	<ul style="list-style-type: none"> • MG scheduling based on chance-constraint programming (CCP) to ensure the reliable operation in islanded mode • Proposed PSI index for successful islanding • 5-interval approximation based on forecast error while all uncertainties are modeled as independent PDFs • Voltage limitation and upper/lower limits of power exchanged are neglected
Ref [25]	<ul style="list-style-type: none"> • PSS index is proposed which shows the probability of self-sufficiency in grid-connected mode, only for a special case.
This paper	<ul style="list-style-type: none"> • RMG scheduling based on chance-constrained goal programming (CCGP) to improve the flexibility of CCP • Proposed PIO denotes the ability of RMG to meet local demand versus the external disturbance • 13-intervals approximation of Gaussian PDF based on the net forecast error considering the correlation between uncertainties • Considering the limitations of power exchange with the mains, switching actions and voltages for more realistic scheduling of RMG in comparison with similar studies

capacity in islanded mode. The proposed approach is developed with chance-constrained islanding capability to guarantee the successful islanding operation with a specified probability. In [26], to demonstrate the microgrid capability for operating in islanded mode, a probability-based concept is proposed. The proposed method is analyzed in presence of forecast errors of demand and wind power generation. In [27], by considering the uncertainties of load demand, price of electricity, and renewable energy, a risk-constrained stochastic framework for autonomous microgrids is proposed. In [28], a robust optimization-based algorithm is developed for optimal scheduling of microgrid operation with islanding capability constraints. With the proper robust level, the proposed microgrid scheduling model with islanding constraints ensures the successful off-grid operation with minimum load shedding.

The review of the literature shows that the scheduling of microgrids in islanded mode has attracted the attention of researchers recently. Nevertheless, the microgrid scheduling with islanding capability is not studied for RMGs as the next generation of microgrids. In this article, chance-constrained goal (CCG) scheduling of an RMG with islanding capability operation is proposed. The probability of islanding operation (PIO) as a successful islanding index is formulated based on the forecast errors of PV and wind power generation as well as load demand. This criterion guarantees the supply of local loads in islanded operation and provides much more flexibility and reliability for microgrid. The main contributions of the article can be summarized as follows.

- 1) Introduction of a new index for islanding operation capability called PIO which represents the capability of microgrid to meet the local load in autonomous operation.
- 2) Formulate the RMG scheduling with islanding constraint as a CCG programming (CCGP).
- 3) Analyze the proposed RMG scheduling for different levels of PIO considering the limitation on the number of switching actions.

For further clarification, article's innovations are compared to similar works in details, which is given in Table I.

The rest of this article is organized as follows. Section II provides the microgrid optimal scheduling problem formulation including objective function and related constraints. The proposed CCG scheduling with islanding capability is introduced in Section III. Section IV presents numerical results and investigates the performance of the proposed model. Finally, Section V concludes the article and draws future works.

II. PROBLEM FORMULATION

This section describes the microgrid optimal scheduling formulation. In the examined microgrid with a number of dispatchable unit (i.e., microturbine), nondispatchable unit (i.e., wind and PV), ESS (i.e., battery), and normally open and close switches, the objective is to minimize the total operation cost in terms of generation cost, purchasing cost of electricity from upstream network, reliability cost, and switching cost. The objective function is given by

$$\begin{aligned} \text{Min} \sum_{t=1}^T & \left(\sum_{i=1}^{NG} (F(p_i)X_{i,t} + SU_{i,t} + SD_{i,t}) + \sum_{t=1}^T \lambda_t P_t^{PCC} \right. \\ & \left. + \sum_{j=1}^J La_j C_j^L \lambda_j + \sum_{t=1}^T \sum_{s=1}^S N_{s,t}^{SW} \lambda^{sw} \right) \end{aligned} \quad (1)$$

where $(F(P_{i,t}))$ is the fuel cost consumption function of the i th MT at the t th time that is calculated as follows [29]:

$$F(P_{i,t}) = a_i + b_i P_{i,t} + c_i (P_{i,t})^2 \quad i \in N, t \in T. \quad (2)$$

The second and the third terms of (1) represent the startup and shutdown cost, respectively. The fourth term represents the purchasing cost of power from the upstream network. As mentioned, the microgrid can exchange power with the mains at PCC. λ_t is a price of purchasing power at the t th time interval. To consider the effect of reliability improvement in the problem formulation, the expected consumer interruption cost as [30] is considered by the introduction of the fifth term in (1). The last term of (1) represents the switching cost. λ^{sw} is the cost of each switching action and $N_{s,t}^{SW}$ is the switching action of the s th switch at the t th time interval. The state of each switch can be either 0 or 1 denoting the open or closed condition, respectively. Therefore, the total numbers of switching actions for the s th switch at the end of the examined period (N_s^{SW}) can be calculated as

$$N_s^{sw} = \sum_{t=1}^T |S_{s,t} - S_{s,t-1}|. \quad (3)$$

The objective function is subject to different constraints as follows:

$$P_i^{\min}(t) \leq P_i(t) \leq P_i^{\max}(t) \quad \forall t \in T, i \in NG \quad (4)$$

$$\text{MUT}_i(X_{i,t} - X_{i,t-1}) \leq T_i^{\text{on}} \quad \forall t \in T, i \in NG \quad (5)$$

$$\text{MDT}_i(X_{i,t-1} - X_{i,t}) \leq T_i^{\text{off}} \quad \forall t \in T, i \in NG \quad (6)$$

$$P_i(t) - P_i(t-1) \leq RU_i \quad \forall t \in T, i \in NG \quad (7)$$

$$P_i(t-1) - P_i(t) \leq RD_i \quad \forall t \in T, i \in NG \quad (8)$$

$$P_i^{\max} X_{i,t} - P_{i,t} \geq R_{i,t}^u \quad \forall t \in T, i \in NG \quad (9)$$

$$P_{i,t} - P_i^{\min} X_{i,t} \geq R_{i,t}^d \quad \forall t \in T, i \in NG \quad (10)$$

$$P_{\text{dis}_b}^{\min}(t) X_{b,t}^d \leq P_b(t) \leq P_{\text{dis}_b}^{\max}(t) X_{b,t}^d \quad \forall t \in T, b \in NB \quad (11)$$

$$P_{\text{char}_b}^{\min}(t) X_{b,t}^c \leq -P_b(t) \leq P_{\text{char}_b}^{\max}(t) X_{b,t}^c \quad \forall t \in T, b \in NB \quad (12)$$

$$X_b^c + X_b^d \leq 1 \quad \forall b \in NB \quad (13)$$

$$T_b^{\text{char}} \geq MC_b (X_{b,t}^c - X_{b,t-1}^c) \quad \forall t \in T, b \in NB \quad (14)$$

$$T_b^{\text{dis}} \geq MD_b (X_{b,t}^d - X_{b,t-1}^d) \quad \forall t \in T, b \in NB \quad (15)$$

$$\text{SOC}^{\min} \leq \text{SOC}_{b,t} \leq \text{SOC}_b^{\max} \quad \forall b \in NB \quad (16)$$

$$P_{\text{dis}_b}^{\max} - P_{b,t} \geq R_{b,t}^u \quad \forall t \in T, b \in NB \quad (17)$$

$$P_{\text{char}_b}^{\max} + P_{b,t} \geq R_{b,t}^d \quad \forall t \in T, b \in NB \quad (18)$$

$$V_j^{\min} \leq V_j \leq V_j^{\max} \quad \forall j \quad (19)$$

$$|I_k| \leq I_k^{\max} \quad \forall k \quad (20)$$

$$N_s^{\text{sw}} \leq N^{\text{sw},\max} \quad \forall s \quad (21)$$

$$P_{Pcc}^{\min}(t) \leq P_{Pcc}(t) \leq P_{Pcc}^{\max}(t) \quad t \in T \quad (22)$$

$$\sum_{i=1}^{NG} P_{i,t} + P_{w,t} + P_{pv,t} + P_{Pcc,t} \pm \sum_{b=1}^{NB} P_{b,t} = \sum_{d=1}^{ND} P_{d,t} \quad \forall t. \quad (23)$$

Constraint (4) represents that generated power by the i th MT is bounded by an upper and a lower limit. The MT must be ON/OFF for a minimum time before it can be shutdown/started up, respectively, as stated in (5) and (6). Constraints (7) and (8) represent the ramp up and ramp down of the i th MT. To have a reliable system operation spinning reserve capacities (both up and down reserves) must be considered. For an unexpected load demand increase, unpredictable collapse in PV or WT power output and/or constrained outage of MT, the up spinning reserve capacity is required to be supplied by the dispatchable units. Similarly, for sudden load demand decrease

and/or unexpected increases in renewable generation unit power output, the down spinning reserve has to be activated [31]. To this end, constraints (9) and (10) represent the up and down spinning reserves, respectively [25]. The charging/discharging power of the battery should also be bounded by certain values as shown in (11) and (12), where $X_{b,t}^d$ and $X_{b,t}^c$ are binary variables for discharging (“0”) or charging (“1”) modes, respectively. The operation modes of the battery are separated by (13). The battery is subject to minimum charging and discharging time limits as (14) and (15) [22]. The battery state of charge (SOC) is presented in (16). Similar to MT, up and down spinning reserves limitations for a battery unit are given in (17) and (18). After reconfiguration, the voltage of each bus must be in an acceptable range as stated in (19). Constraint (20) shows the branch current constraint. The total number of switching actions during reconfiguration that is calculated in (3) is limited by (21). The power purchased is bounded by upper and lower limits as (22). Finally, (23) denotes the supply–demand power balance constraint, where NG , NB , and ND are the number of MTs, batteries, and load, respectively.

III. OPTIMAL SCHEDULING OF RMG WITH PROBABILITY ISLANDING OPERATION (PIO) CONSTRAINT

The general form of chance-constraint programming (CCP) is formulated as

$$\Pr \{f_i(x, \xi) \leq b_i\} \leq B_i \quad (24)$$

where B_i is the confidence level, x is a set of decision variables, ξ is a set of uncertain parameters, and b_i is a value of objective function (f). In the CCP, the probability of changes of uncertain parameters cannot exceed a predetermined level. Therefore, to improve the flexibility of CCP, it is reformed to the CCGP as

$$\Pr \{f_i(x, \xi) - b_i \geq d_i^+\} \geq B_i^+ \quad (25)$$

$$\Pr \{b_i - f_i(x, \xi) \leq d_i^-\} \geq B_i^- \quad (26)$$

where d_i^+ and d_i^- are positive deviations from the value of target.

As mentioned, PV and WT power output, as well as load demand forecast, are prone to errors. The forecast error of WT power output (ΔP_w), PV power output (ΔP_{pv}), and forecast error of load demand (ΔP_d) can be characterized as independent Gaussian distributed random variables. All three uncertain parameters are the result of real value and a prediction error. The value of net forecast demand is the result of subtracting the load consumption and total power generated by the renewable units, which can be represented as

$$P_{d_F}^t = P_{d_A}^t - P_{PVA}^t - P_{WA}^t + \Delta e_t^N \quad (27)$$

where P_{PVA}^t , P_{WA}^t , and $P_{d_A}^t$ are actual PV, wind power output, and load demand, Δe_t^N is a net error which is a combination of PV and wind, as well as, load demand forecast errors. Given that the forecasted errors of all uncertain parameters are unrelated,

the standard deviation of net error can be calculated as

$$\sigma_t^N = \sqrt{(\sigma_{P_d}^t)^2 + (\sigma_{P_{pv}}^t)^2 + (\sigma_{P_w}^t)^2}. \quad (28)$$

As [32], the standard deviation of load forecasted error is a percentage of actual load demand in whole forecasting horizon

$$\sigma_{P_d}^t = \frac{k}{100} P_{d_A}^t \quad (29)$$

where k is a function of the predication accuracy percentage. The standard deviation of wind and PV power output forecast errors can be approximated as

$$\sigma_{P_{pv}}^t = \frac{1}{5} P_{PV_F}^t + \frac{1}{50} P_{PV_I}^t \quad (30)$$

$$\sigma_{P_w}^t = \frac{1}{5} P_{w_F}^t + \frac{1}{50} P_{w_I}^t \quad (31)$$

where I and F symbol represent the total installation capacity and forecasted value of wind and PV unit.

According to the above description, the net forecast error can be represented by Gaussian distribution

$$\Delta e_t^N (\mu_t^N, \sigma_t^N). \quad (32)$$

To guarantee adequate spinning reserves for an islanding operation, the following constraint should be considered:

$$\begin{aligned} & -\sum_{i=1}^{NG} R_{i,t}^d - \sum_{b=1}^{NB} R_{b,t}^d - P_{Pcc,t} \leq \Delta e_t^N \\ & \leq \sum_{i=1}^{NG} R_{i,t}^u + \sum_{b=1}^{NB} R_{b,t}^u - P_{Pcc,t}. \end{aligned} \quad (33)$$

Based on (25) and (26), the reserve CCGP constraints considering up and down spinning reserves are reformed as

$$\Pr \left\{ \sum R_{i,t}^{\text{up}} + \sum R_{b,t}^{\text{up}} - P_{pcc,t} \geq \Delta e_t^N \right\} \geq B_t^{\text{up}} \quad (34)$$

$$\Pr \left\{ -\sum R_{i,t}^{\text{down}} - \sum R_{b,t}^{\text{sown}} - P_{pcc,t} \leq \Delta e_t^N \right\} \geq B_t^{\text{down}}. \quad (35)$$

The amount of required reserve that guarantees the operation of RMG in the islanded mode and represents the successful islanding operation can be approximated by dividing the net error probability distribution to the 13 intervals. Fig. 1 depicts the Gaussian distribution function of net error which consists of 13 intervals. Each interval is associated with a probability like π_c . The probability of a scenario occurrence in the c th interval with the upper and lower bands can be assessed as

$$\pi_c = \int_{l_b}^{u_b} \frac{1}{\sigma_t^N \sqrt{2\pi}} e^{-\frac{(x-\mu_t^N)^2}{2\sigma_t^{N^2}}} dx = \frac{1}{2} \text{erf} \left(\frac{x-\mu_t^N}{\sqrt{2}\sigma_t^N} \right) \Big|_{l_b}^{u_b} \quad (36)$$

where l_b and u_b are the lower and upper band of each interval, respectively. For 13-interval approximation (see Fig. 1), l_b and

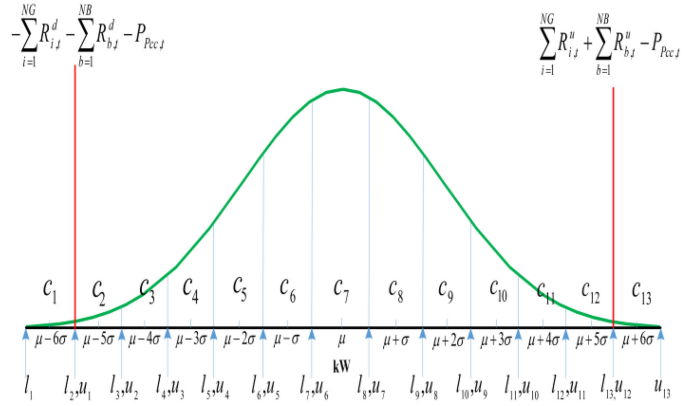


Fig. 1. Thirteen-interval Gaussian distribution approximation based on net forecast error.

u_b are calculated as

$$l_b = \left(\mu_t^N - \frac{(c-7)}{\sigma_t^N} \right) - \frac{1}{2} \sigma_t^N \quad c = 1, 2, \dots, 13 \quad (37)$$

$$u_b = \left(\mu_t^N - \frac{(c-7)}{\sigma_t^N} \right) + \frac{1}{2} \sigma_t^N \quad c = 1, 2, \dots, 13. \quad (38)$$

It should be noted that the larger number of intervals increases the accuracy while demanding a larger computational requirement. Whenever the probability of net error, which is a function of up and down spinning reserve as well as a power exchanged with the upstream network, is between the negative and positive changes (25–26), a sufficient reserve for successful islanding operation is guaranteed. In other words, the area between d^- and d^+ axes (which are determined by the value of reserves and exchanged power) indicates the PIO. To recognize intervals which denote the islanding capability, binary variable v_c^t is introduced. Then

$$\text{PIO} = \sum_{c=1}^{N_c} v_c^t \times \pi_c^t \quad \text{and} \quad \text{PIO} \geq \text{PIO}^{\text{target}} \quad (39)$$

where $v_c^t = \phi_{u_c}^t - \phi_{l_c}^t$. $\phi_{u_c}^t$ and $\phi_{l_c}^t$ are auxiliary binary variables which are associated with realization of net forecast error and calculated as

$$\phi_{u_c}^t = \begin{cases} 1 & \text{if } u_{b_c} \leq \sum R_{i,t}^{\text{up}} + \sum R_{b,t}^{\text{up}} - P_{pcc,t} \\ 0 & \text{otherwise} \end{cases} \quad (40)$$

$$\phi_{l_c}^t = \begin{cases} 1 & \text{if } l_{b_c} \leq -\sum R_{i,t}^{\text{up}} - \sum R_{b,t}^{\text{up}} - P_{pcc,t} \\ 0 & \text{otherwise.} \end{cases} \quad (41)$$

The proposed PIO index based on CCGP provides the microgrid operator with an opportunity for scheduling after temporary islanding with definite probability.

IV. NUMERICAL SIMULATION

The proposed chance-constrained RMG scheduling with islanding capability, which was introduced in Sections II and III, is implemented on a 10-bus test system [7]. The single-line diagram of the examined system is depicted in Fig. 2.

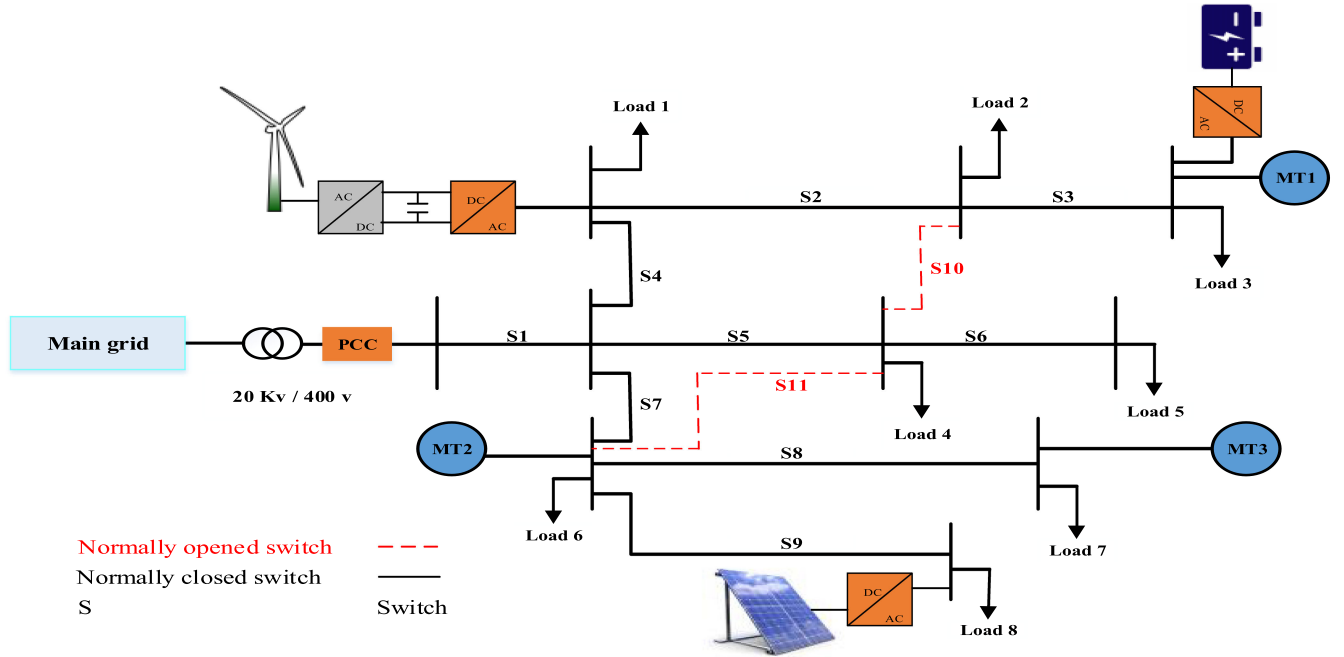


Fig. 2. Structure of the 10-bus RMG test system.

TABLE II
PARAMETERS OF BATTERY-BASED ESS [25]

	SOC^{min} / SOC^{max} (%)	Capacity (kWh)	Min- Max char(dis) power (kW)	Min char(dis) time (h)
Value	15 - 85	100	50	2

TABLE III
PARAMETERS OF MICROTURBINES [26]

Unit	Min power (kW)	Max power (kW)	Startup/shut down cost (\$)	a (\$)	b (\$/kW)	c (\$ / kw^2)
MT1	30	100	45	1.3	0.0304	0.000104
MT2	75	150	2.5	0.38	0.0267	0.00024
MT3	75	150	2.5	0.38	0.0267	0.00024

As can be seen, the modified test system includes multiple resources, such a PV farm, a wind turbine, a battery-based ESS, and three microturbines. There are 11 switches in the network, and due to the radial structure, two of them should be open at any time. To establish this limitation, the bus incidence matrix is implemented.

The characteristic of battery and MTs are given in Tables II and III, respectively.

The 120-kW WT is considered according to [33]. Based on forecast results of wind speed, the corresponding power generated by WT is calculated, which is shown in Fig. 3. Also, as in [34], the irradiation and temperature data are used to calculate the generated power of a 150-kW PV farm which is shown in Fig. 3.

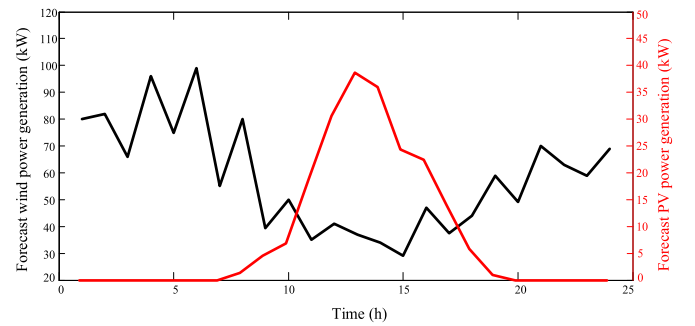


Fig. 3. Forecasted power generation of a 120-kW wind turbine and 150-kW PV panel.

The forecast error of renewable sources (WT and PV) power output are modeled by independent normal distributions with zero mean and 10% standard deviation. The forecasted load demand is given in Table IV. As another uncertain parameter, the forecast error of load demand is subject to the normal distribution with 2% standard deviation and zero mean. The day-ahead market price is also given in Table IV.

The maximum number of switching action for each switch is considered to be ten actions per day. Also, the cost of each switching action is \$1. Computer simulations and required coding are carried out in MATLAB software and using CPLEX 11.2 solver. To find the optimal topology of the system, time-varying acceleration coefficients particle swarm optimization (TVAC-PSO) algorithm is used [7], [35].

To conduct the stochastic study, 1000 scenarios are generated by using Monte Carlo simulation for PV, WT, as well as, load demand. For each scenario, the power exchange at PCC is

TABLE IV
FORECASTED LOAD DEMAND AND DAILY MARKET PRICE

Time (h)	Load (kW)	Power price (cent/kWh)	Time (h)	Load (kW)	Power price (cent/kWh)
1	260.731	9.36	13	397.74	27.12
2	262.059	7.59	14	400.863	25.89
3	279.805	6.99	15	391.64	26.41
4	288.317	7.02	16	374.25	18.501
5	280.921	8.51	17	362.569	16.23
6	307.804	8.96	18	379.042	12.96
7	319.723	9.01	19	389.85	15.62
8	322.903	10.68	20	425.492	21.56
9	328.745	11.27	21	447.642	29.65
10	340.357	14.52	22	399.201	31.175
11	379.24	18.23	23	370.856	18.7
12	387.974	23.61	24	281.421	10.23

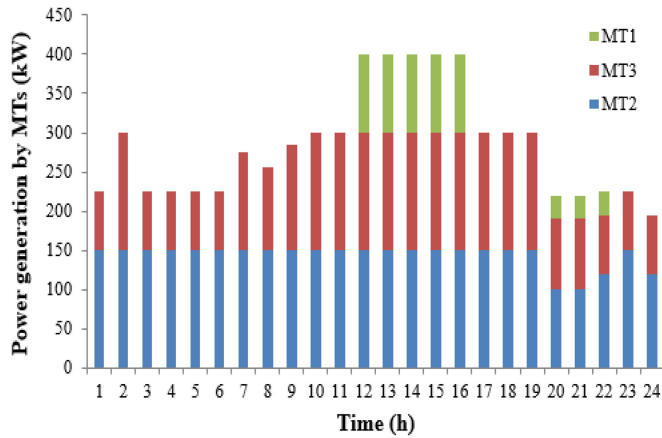


Fig. 4. MTs power dispatch for 24 h with $PIO = 0.999$.

calculated based on forecast error of PV, WT, and load demand and the islanding condition is examined.

To demonstrate the effectiveness of the proposed chance-constrained scheduling, simulation results are presented for two cases. In the first case, the microgrid scheduling is analyzed with $PIO^{\text{target}} = 0.999$. In the second case, RMG scheduling is done with different levels of probability of islanding operation.

A. Chance-Constrained Scheduling of RMG With $PIO = 0.999$

In this case, the microgrid scheduling is done with $PIO^{\text{target}} = 0.999$, this value equals $12\sigma_t$. The optimal scheduling of MTs is depicted in Fig. 4. As can be seen from Fig. 4, MT 1 is committed only in pick-load hours (12–16 and 20–22 P.M.) due to its higher cost of operation.

Table V shows the normally open switches (NO) at any hour. It can be seen that to satisfy the radial structure of the system, two switches should be open at any hour.

Also, Table V shows the battery state for 24 h. It should be noted that charging, discharging, and idle states of battery are represented by -1 , 1 , and 0 , respectively.

Fig. 5 shows the total amount of up/down spinning reserve of dispatchable units (MTs and battery). As can be seen, up

TABLE V
RESULT OF RECONFIGURATION WITH $PIO = 0.999$

Time (h)	Open switches	Battery state	Time (h)	Open switches	Battery state
1	s_4, s_7	-1	13	s_5, s_{11}	+1
2	s_4, s_7	-1	14	s_5, s_{11}	+1
3	s_4, s_7	-1	15	s_5, s_{11}	+1
4	s_4, s_7	-1	16	s_4, s_7	0
5	s_5, s_{11}	-1	17	s_4, s_7	-1
6	s_5, s_{11}	0	18	s_4, s_7	-1
7	s_5, s_{11}	0	19	s_4, s_7	+1
8	s_5, s_{11}	0	20	s_4, s_{10}	+1
9	s_4, s_{10}	0	21	s_4, s_{10}	+1
10	s_4, s_{10}	0	22	s_4, s_{10}	0
11	s_4, s_{10}	0	23	s_4, s_{10}	0
12	s_4, s_{10}	+1	24	s_4, s_{10}	-1

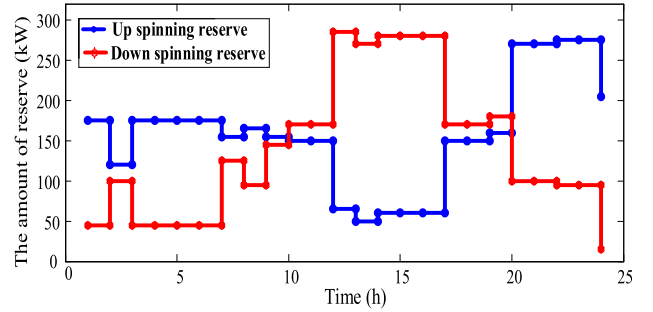


Fig. 5. Amount of up/down spinning reserve with $PIO = 0.999$.

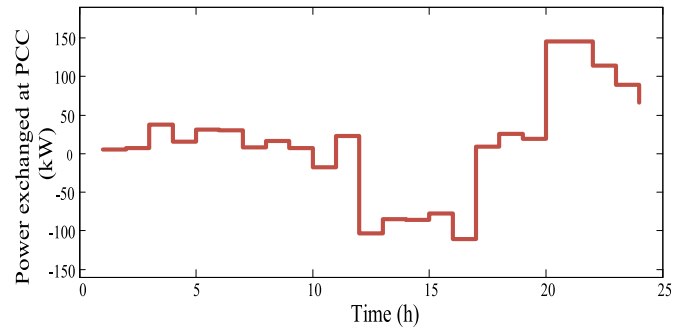


Fig. 6. Power exchanged between RMG and upstream network at PCC with $PIO = 0.999$.

and down spinning reserves have different behaviors. Up spinning reserve is considered for compensation of unexpected load increase. Therefore, when microgrid imports more energy from upstream network, up spinning reserve should be at higher values to secure the operation in case of an unintentional islanding event.

Also, the down spinning reserve, which is considered for compensation of fluctuation in PV and WT power generation, should be equal to its high value when there is surplus power and the microgrid can sell power to the upstream network.

TABLE VI
RESULT OF RECONFIGURATION AND BATTERY OPERATION FOR
DIFFERENT LEVELS OF PIO

Hour	PIO=70%		PIO=80%		PIO=90%	
	NO	Battery state	NO	Battery state	NO	Battery state
1	s_4, s_5	-1	s_7, s_{11}	-1	s_7, s_{11}	-1
2	s_4, s_5	-1	s_7, s_{11}	-1	s_7, s_{11}	-1
3	s_4, s_5	-1	s_7, s_{11}	-1	s_5, s_7	-1
4	s_{10}, s_{11}	0	s_4, s_5	0	s_5, s_7	-1
5	s_{10}, s_{11}	0	s_4, s_5	0	s_5, s_7	-1
6	s_{10}, s_{11}	0	s_4, s_5	0	s_5, s_7	0
7	s_{10}, s_{11}	0	s_5, s_{10}	-1	s_5, s_7	0
8	s_{10}, s_{11}	-1	s_5, s_{10}	-1	s_7, s_{11}	-1
9	s_{10}, s_{11}	-1	s_5, s_{10}	0	s_7, s_{11}	-1
10	s_{10}, s_{11}	-1	s_5, s_{10}	0	s_{10}, s_{11}	0
11	s_{10}, s_{11}	0	s_5, s_{10}	0	s_{10}, s_{11}	0
12	s_{10}, s_{11}	0	s_5, s_{10}	+1	s_4, s_{11}	+1
13	s_{10}, s_{11}	+1	s_5, s_{10}	+1	s_4, s_{11}	+1
14	s_{10}, s_{11}	+1	s_5, s_{10}	+1	s_4, s_{11}	+1
15	s_{10}, s_{11}	+1	s_5, s_{10}	+1	s_4, s_{11}	+1
16	s_4, s_5	0	s_4, s_5	0	s_4, s_{11}	0
17	s_4, s_5	0	s_4, s_5	0	s_5, s_{10}	-1
18	s_4, s_5	0	s_4, s_5	-1	s_5, s_{10}	-1
19	s_4, s_5	0	s_4, s_5	-1	s_5, s_{10}	0
20	s_7, s_{11}	0	s_5, s_{10}	+1	s_5, s_{10}	0
21	s_7, s_{11}	+1	s_{10}, s_{11}	+1	s_7, s_{11}	+1
22	s_7, s_{11}	+1	s_{10}, s_{11}	0	s_7, s_{11}	+1
23	s_7, s_{11}	0	s_{10}, s_{11}	0	s_7, s_{11}	0
24	s_7, s_{11}	0	s_{10}, s_{11}	0	s_7, s_{11}	0

Fig. 6 shows the exchanged power at PCC between RMG and upstream network. Comparing the results shown in Figs. 5 and 6 proves the relationship between up/down spinning reserve and power exchanged at PCC. For example, at 20–23 P.M. when the high power is injected from the upstream network, up spinning reserve reaches its highest value. Also, at 12–16 P.M., when the microgrid sells the high amount of power to the upstream network, the value of down spinning reserve reaches its highest value.

B. Chance-Constrained Scheduling of RMG With Different PIO Levels

To demonstrate the effect of islanding criterion (PIO) on microgrid scheduling, RMG scheduling with different levels of PIO are analyzed and compared in this section.

Fig. 7 shows the generated power by MTs. In scheduling with high level of PIO [see Fig. 7(c)], MTs are committed more frequently than the situations with lower levels of PIO [see Fig. 7(a) and (b)]. Obviously, at higher PIOs, to maintain a suitable level of reliability, local units should be committed at more times and generate more power compared to the scheduling with PIO = 70 and 80%. Table VI represents the normally open switches for three different values of PIO. As can be seen, with increasing PIO, the change in topology of the microgrid is increasing. In other words, at higher PIOs, where the probability of interruption of local load is nearly one, the microgrid should have an optimal structure. By applying appropriate switching

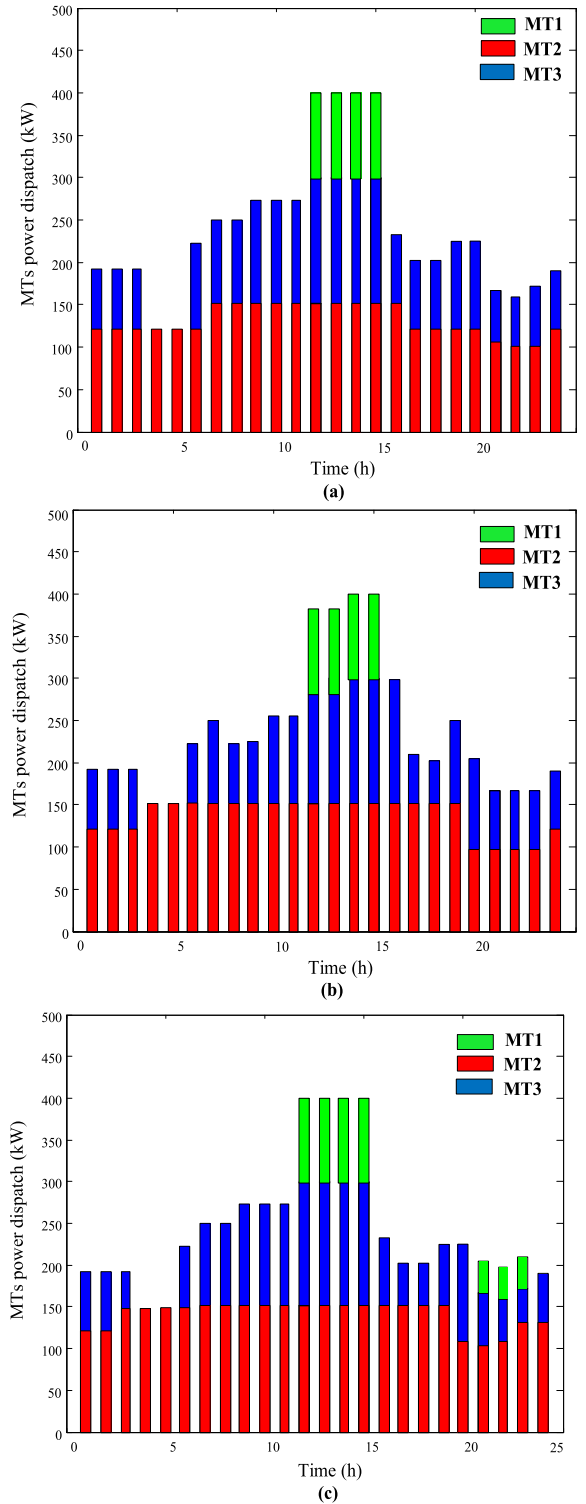


Fig. 7. MTs power dispatch for 24 h with (a) PIO = 70%, (b) PIO = 80%, and (c) PIO = 90%.

actions, it is possible to minimize power losses through optimal power rerouting. However, it should be noted that with the increasing PIO value, the number of switching action is also increasing. Also, Table VI illustrates the battery operation for the different levels of PIO. As can be seen, with the increasing PIO value, variation in the amount of energy stored in battery also

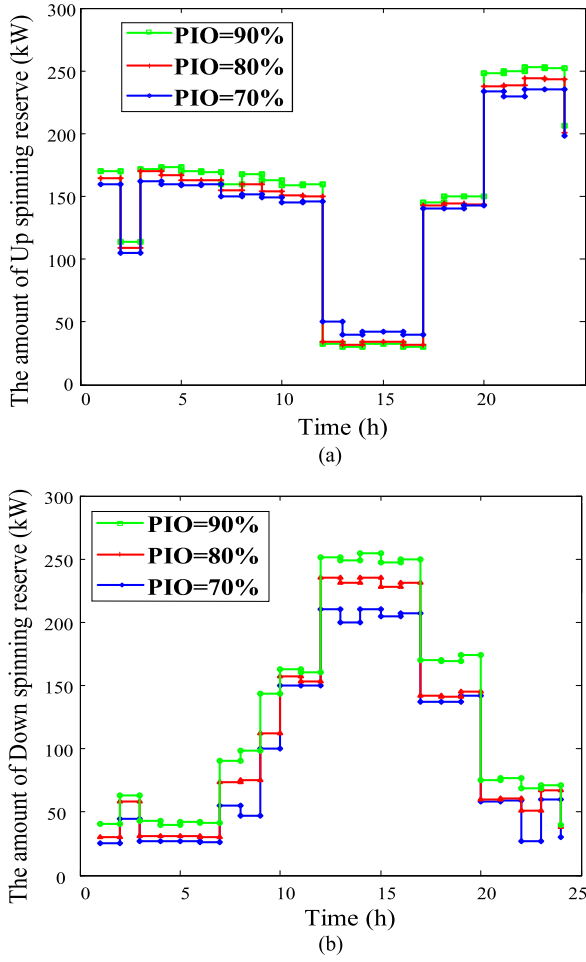


Fig. 8. Amount of (a) up spinning reserve and (b) down spinning reserve with different levels of PIO.

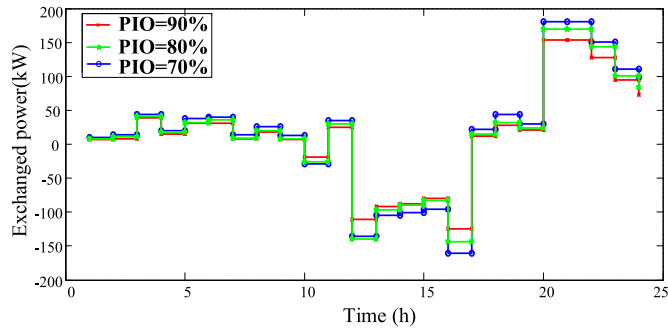


Fig. 9. Power exchanged between the RMG and the upstream network at different levels of PIO.

increases. At higher levels of PIO, when the microgrid needs more energy supplement, the battery discharges more frequently compared to cases with lower levels of PIO. In this regard, the idle time of battery is less once the PIO is higher.

Figs. 8 and 9 show the amount of up/down spinning reserve and exchanged power at PCC for the different levels of PIO, respectively. As can be seen, with increasing PIO, the amount of up/down spinning reserve is increasing. Also, with increasing

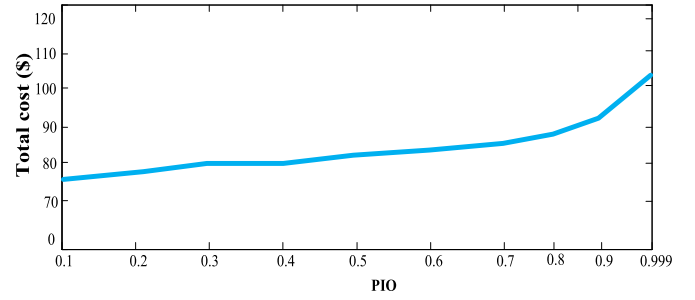


Fig. 10. Total operation cost of RMG for different levels of PIO.

PIO, the amount of power exchanged at PCC is decreasing. By increasing the value of PIO, when the value of up/down spinning reserve reaches its highest value (20–23 P.M. and 12–15 P.M.), i.e., in $\text{PIO} = 90\%$, power exchanged at PCC decreases.

Finally, the total cost of RMG scheduling with different levels of PIO is depicted in Fig. 10. As observed, with the increasing value of PIO, microgrid total cost increases. Increase in the total cost is less at lower levels of PIO (6.41% for PIO increases from 0.1 to 0.7). Once the PIO is higher (from 0.8 to 0.999), the slope of PIO is greater. It illustrates that while microgrids have adequate power to meet the local load and reliability is high, small increase of reliability level will need a remarkable increase of total cost. However, the increase in total cost of microgrid is negligible compared to the multiple advantages created by increasing PIO.

V. CONCLUSION

In this article, a new strategy for scheduling of RMGs with related constraints was presented. A new islanding operation index named PIO was considered to measure the probability of successful islanding operation and show that microgrid has an adequate level of spinning reserve to meet the local loads during the off-grid operation. The proposed scheduling was formulated as a chance-constrained global optimization problem and using the 13-interval approximation method, taking into account the forecast errors of PV and wind power generation, as well as, load demand. Simulation results were presented for different levels of PIO. Numerical results showed that by increasing the value of PIO, power generated by dispatchable units, the value of up and down spinning reserves and changes in microgrid structure are increased. Also, at the high value of PIO when microgrid transacts high amount of power with upstream network, the values of reserves are increased. At these times, the value of up and down spinning reserve reaches the highest values. Monetary results showed that by increasing the value of PIO, the total cost increases. The percentage increase of total cost is greater once the value of PIO is higher. This represents that a small increase of reliability level demands a remarkable increase in total system costs while the reliability is already high.

In this article, it is assumed that the electricity price is already known and does not include the uncertain parameters. The efficiency of the proposed method will be further improved by considering the uncertainty of power price and integration

of demand response program in regional RMGs. Moreover, reliability assessment from different reliability index points of view is left to future work.

REFERENCES

- [1] N. Hatziaargyriou, *Microgrids: Architectures and Control*. Hoboken, NJ, USA: Wiley, 2014.
- [2] M. S. Purser, "A technical and economic feasibility study of implementing a microgrid at Georgia Southern University," M.S. thesis, Dept. Mech. Eng., Georgia Southern Univ., 2014.
- [3] F. S. Gazijahani and J. Salehi, "Robust design of microgrids with reconfigurable topology under severe uncertainty," *IEEE Trans. Sustain. Energy*, vol. 9, no. 2, pp. 559–569, Apr. 2018.
- [4] C. Wang *et al.*, "A highly integrated and reconfigurable microgrid testbed with hybrid distributed energy sources," *IEEE Trans. Smart Grid*, vol. 7, no. 1, pp. 451–459, Jan. 2016.
- [5] A. Kavousi-Fard, A. Khodaei, and S. Bahramirad, "Improved efficiency, enhanced reliability and reduced cost: The transition from static microgrids to reconfigurable microgrids," *Elect. J.*, vol. 29, pp. 22–27, 2016.
- [6] S. Golshannavaz, S. Afsharnia, and P. Siano, "A comprehensive stochastic energy management system in reconfigurable microgrids," *Int. J. Energy Res.*, vol. 40, pp. 1518–1531, 2016.
- [7] M. Hemmati, B. Mohammadi-Ivatloo, S. Ghasemzadeh, and E. Reihani, "Risk-based optimal scheduling of reconfigurable smart renewable energy based microgrids," *Int. J. Elect. Power Energy Syst.*, vol. 101, pp. 415–428, 2018.
- [8] M. Bornapour, R.-A. Hooshmand, A. Khodabakhshian, and M. Parastegari, "Optimal stochastic scheduling of CHP-PEMFC, WT, PV units and hydrogen storage in reconfigurable micro grids considering reliability enhancement," *Energy Convers. Manage.*, vol. 150, pp. 725–741, 2017.
- [9] M. Hemmati, S. Ghasemzadeh, and B. Mohammadi-Ivatloo, "Optimal scheduling of smart reconfigurable neighbour micro-grids," *IET Gener., Transmiss. Distrib.*, vol. 13, no. 3, pp. 380–389, 2019. [Online]. Available: <https://digital-library.theiet.org/content/journals/10.1049/iet-gtd.2018.6388>
- [10] T. Ding, Y. Lin, Z. Bie, and C. Chen, "A resilient microgrid formation strategy for load restoration considering master-slave distributed generators and topology reconfiguration," *Appl. Energy*, vol. 199, pp. 205–216, 2017.
- [11] R. Jabbari-Sabet, S.-M. Moghaddas-Tafreshi, and S.-S. Mirhoseini, "Microgrid operation and management using probabilistic reconfiguration and unit commitment," *Int. J. Elect. Power Energy Syst.*, vol. 75, pp. 328–336, 2016.
- [12] M. Nazari-Heris, B. Mohammadi-Ivatloo, G. B. Gharehpetian, and M. Shahidehpour, "Robust short-term scheduling of integrated heat and power microgrids," *IEEE Syst. J.*, vol. 13, no. 3, pp. 3295–3303, Sep. 2019.
- [13] J. Liu, H. Chen, W. Zhang, B. Yurkovich, and G. Rizzoni, "Energy management problems under uncertainties for grid-connected microgrids: A chance constrained programming approach," *IEEE Trans. Smart Grid*, vol. 8, no. 6, pp. 2585–2596, Nov. 2017.
- [14] Z. Shi, H. Liang, S. Huang, and V. Dinavahi, "Distributionally robust chance-constrained energy management for islanded microgrids," *IEEE Trans. Smart Grid*, vol. 10, no. 2, pp. 2234–2244, Mar. 2019.
- [15] M. Hemmati, B. Mohammadi-Ivatloo, and A. Soroudi, "Uncertainty management in decision-making in power system operation," in *Decision Making Applications in Modern Power Systems*. New York, NY, USA: Elsevier, 2020, pp. 41–62.
- [16] Y. Xiang, J. Liu, and Y. Liu, "Robust energy management of microgrid with uncertain renewable generation and load," *IEEE Trans. Smart Grid*, vol. 7, no. 2, pp. 1034–1043, Mar. 2016.
- [17] O. Ciftci, M. Mehrtash, F. Safdarian, and A. Kargarian, "Chance-constrained microgrid energy management with flexibility constraints provided by battery storage," in *Proc. IEEE Texas Power Energy Conf.*, 2019, pp. 1–6.
- [18] X. Cao, J. Wang, and B. Zeng, "Networked microgrids planning through chance constrained stochastic conic programming," *IEEE Trans. Smart Grid*, vol. 10, no. 6, pp. 6619–6628, Nov. 2019.
- [19] E. Craparo, M. Karatas, and D. I. Singham, "A robust optimization approach to hybrid microgrid operation using ensemble weather forecasts," *Appl. Energy*, vol. 201, pp. 135–147, 2017.
- [20] X. Cao, J. Wang, and B. Zeng, "A chance constrained information-gap decision model for multi-period microgrid planning," *IEEE Trans. Power Syst.*, vol. 33, no. 3, pp. 2684–2695, May 2018.
- [21] A. Ravichandran, S. Sirouspour, P. Malysz, and A. Emadi, "A chance-constraints-based control strategy for microgrids with energy storage and integrated electric vehicles," *IEEE Trans. Smart Grid*, vol. 9, no. 1, pp. 346–359, Jan. 2018.
- [22] A. Khodaei, "Microgrid optimal scheduling with multi-period islanding constraints," *IEEE Trans. Power Syst.*, vol. 29, no. 3, pp. 1383–1392, May 2014.
- [23] T. Ding, K. Sun, C. Huang, Z. Bie, and F. Li, "Mixed-integer linear programming-based splitting strategies for power system islanding operation considering network connectivity," *IEEE Syst. J.*, vol. 12, no. 1, pp. 350–359, Mar. 2018.
- [24] D. Michaelson, H. Mahmood, and J. Jiang, "Reduction of forced outages in islanded microgrids by compensating model uncertainties in PV rating and battery capacity," *IEEE Power Energy Technol. Syst. J.*, vol. 5, no. 4, pp. 129–138, Dec. 2018.
- [25] G. Liu, M. Starke, B. Xiao, X. Zhang, and K. Tomsovic, "Microgrid optimal scheduling with chance-constrained islanding capability," *Elect. Power Syst. Res.*, vol. 145, pp. 197–206, 2017.
- [26] B. Zhao, Y. Shi, X. Dong, W. Luan, and J. Bornemann, "Short-term operation scheduling in renewable-powered microgrids: A duality-based approach," *IEEE Trans. Sustain. Energy*, vol. 5, no. 1, pp. 209–217, Jan. 2014.
- [27] M. Vahedipour, A. Anvari-Moghaddam, and J. Guerrero, "Evaluation of reliability in risk-constrained scheduling of autonomous microgrids with demand response and renewable resources," *IET Renewable Power Gener.*, vol. 12, no. 6, pp. 657–667, 2018.
- [28] G. Liu, M. Starke, B. Xiao, and K. Tomsovic, "Robust optimisation-based microgrid scheduling with islanding constraints," *IET Gener., Transmiss. Distrib.*, vol. 11, pp. 1820–1828, 2017.
- [29] H. Sadeghian and M. Ardehali, "A novel approach for optimal economic dispatch scheduling of integrated combined heat and power systems for maximum economic profit and minimum environmental emissions based on Benders decomposition," *Energy*, vol. 102, pp. 10–23, 2016.
- [30] A. Kavousi-Fard and A. Khodaei, "Efficient integration of plug-in electric vehicles via reconfigurable microgrids," *Energy*, vol. 111, pp. 653–663, 2016.
- [31] T.-Y. Lee, "Optimal spinning reserve for a wind-thermal power system using EIPSO," *IEEE Trans. Power Syst.*, vol. 22, no. 4, pp. 1612–1621, Nov. 2007.
- [32] M. A. Ortega-Vazquez and D. S. Kirschen, "Estimating the spinning reserve requirements in systems with significant wind power generation penetration," *IEEE Trans. Power Syst.*, vol. 24, no. 1, pp. 114–124, Feb. 2009.
- [33] [Online]. Available: <https://en.wind-turbine-models.com/turbines/592-bonus-b19-120>
- [34] [Online]. Available: http://midcdmz.nrel.gov/srrl_bms/
- [35] B. Mohammadi-Ivatloo, M. Moradi-Dalvand, and A. Rabiee, "Combined heat and power economic dispatch problem solution using particle swarm optimization with time varying acceleration coefficients," *Elect. Power Syst. Res.*, vol. 95, pp. 9–18, 2013.